SAE TECHNICAL PAPER SERIES

1999-01-0637

Use of Repeated Crash-Tests to Determine Local Longitudinal and Shear Stiffness of the Vehicle Front with Crush

Dagmar G. Buzeman-Jewkes and Per Lövsund
Chalmers University of Technology

David C. Viano
General Motors Corporation

Reprinted From: Occupant Protection (SP-1432)

The Engineering Society For Advancing Mobility Land Sea Air and Space® INTERNATIONAL

International Congress and Exposition
Detroit, Michigan
March 1-4, 1999

400 Commonwealth Drive, Warrendale, PA 15096-0001 U.S.A. Tel: (724) 776-4841 Fax: (724) 776-5760

ISSN 0148-7191

Printed in USA

1999-01-0637

Use of Repeated Crash-Tests to Determine Local Longitudinal and Shear Stiffness of the Vehicle Front with Crush

Dagmar G. Buzeman-Jewkes and Per Lövsund
Chalmers University of Technology

David C. Viano
General Motors Corporation

ABSTRACT

Crash-test-data on local longitudinal and shear stiffness of the vehicle front is needed to estimate impact severity from car deformation in offset or pole impacts, and to predict vehicle acceleration and compartment intrusion in car-to-car crashes. Repeated full frontal crash-tests were carried out with a load-cell barrier to determine the local longitudinal stiffness with increasing crush. Repeated offset tests were run to determine shear stiffness. Two single high-speed tests (full frontal and offset) were carried out and compared to the repeated tests to determine the rate sensitivity of the front structure. Four repetitions at 33.4 km/h provided equivalent energy absorption to a single 66.7 km/h test, when rebound was considered. Power-train inertial effects were estimated from high-speed tests with and without power-train.

Speed effects averaged 2% per [m/s] for crush up to power-train impact, and post-crash measurements were a reasonable estimate of front-structure stiffness. Power-train inertia significantly increased the barrier force in the high-speed crashes. The repeated tests provide local longitudinal and shear stiffness estimates of the vehicle front structure with deformation in an effective and inexpensive way. The results are useful data for compatibility and accident reconstruction purposes, especially in cases of non-distributed frontal crush. The test method also assesses mass and stiffness aggressivity.

INTRODUCTION

Car occupant injuries are related to interior impacts and restraining loads, which are influenced by passenger compartment acceleration and intrusion. These vehicle responses depend on the impact speed, and on the mass and stiffness of the impacting structures. Stiffness is a necessary parameter for accident reconstruction applications, but can also be used to determine compatibility between passenger cars in car-to-car impacts.

Campbell (1974) was one of the first researchers who measured the stiffness of vehicle fronts. He assumed the stiffness to be uniform over the front width. In reality however, the front stiffness varies over the car width and crush depth (Hobbs et al. 1996). Warner et al. (1986) and Prasad (1990) ran crash tests repeatedly with one vehicle, and estimated front stiffness with increasing crush from post-crash deformation measurements. However, dynamic vehicle characteristics like hysteresis, or maximum crush and intrusion, can only be estimated roughly from post-crash data (Warner et al. 1986). These parameters are needed to predict vehicle rebound and occupant ride-down. Real-time measurements can evaluate post-crash estimates of dynamic parameters.

Local stiffness data are needed to better determine crash severity from car deformation in offset or pole impacts, and to predict vehicle acceleration and intrusion in car-to-car crashes. These data are basic for estimating vehicle and occupant responses in simulations of real-world crashes. Nilsson-Ehle et al. (1982) and Jansson (1982) measured local stiffness of the vehicle front in full frontal crash-tests using a 6 load-cell barrier. Additionally, they ran frontal offset crash tests to determine the shear forces that contribute to the absorption of crash energy in non-distributed frontal collisions. However, they did not determine effects of crush rate-sensitivity and power-train inertia on stiffness. No local stiffness data is available on present car models for use in accident reconstruction or compatibility research.

Local stiffness data of vehicle fronts is indispensable to investigate the influence of vehicle crush characteristics on accident and injury severity, and to improve the quality of accident reconstruction. The purpose of this study was to determine local longitudinal and shear stiffness of the vehicle front with crush. The study was also conducted to evaluate the use of post-crash data, and to determine the rate sensitivity of front structure and power-train inertia effects. The local stiffness data improves the quality of compatibility research and of accident reconstruction in a wide range of frontal collisions.

METHOD

Six full frontal (distributed) and four offset frontal crash-tests were carried out with a load-cell barrier. Four frontal and three offset tests were run repeatedly on the same vehicle, to measure local longitudinal and shear stiffness with crush. Additionally, two high-speed tests were run in a full frontal and 50% offset configuration to determine rate sensitivity of the front structure and to evaluate if superposition of repeated tests could approximate a high-speed crash. The total barrier force in the offset tests was compared with the force of the corresponding barrier-half in full frontal collisions to estimate shear forces. A high speed full frontal test without power-train was performed to study power-train influences.

IMPACT SPEED AND SET-UP FOR REPEATED TESTS – Repeated crash-tests were carried out with SAAB 900 cars in full frontal and 50% offset configuration. Four test repetitions were used to measure impact force, and front structure and compartment deformations post-crash with crush depth. The repeated tests can be superimposed to approximate force-deflection behavior of the vehicle in a high-speed test, in case their equivalent barrier energies are equal. The equivalent barrier energy, EBE, is calculated as the total absorbed energy, E_{abs}, plus the restitution energy of the last test repetition (eq. I, Warner et al. 1986), where the total absorbed energy equals the impact kinetic energy, 1/2 mV_{imp}^2, minus the restitution energy, 1/2 mV_{rest}^2, summed over n test repetitions (eq. II). The parameters m, Vimp and Vrest represent the vehicle mass, impact speed and restitution velocity respectively.

$$EBE = \sum_i^n \frac{1}{2} m(V_{imp}^2 - V_{rest}^2)_i + \frac{1}{2}(mV_{rest}^2)_n \qquad \text{(I)}$$

$$E_{abs} = \sum_i \frac{1}{2} m(V_{imp}^2 - V_{rest}^2)_i \qquad \text{(II)}$$

The speed of the high-speed full frontal test was aimed at about 65.0 km/h to ensure significant compartment intrusion. The impact speed of the repeated tests was estimated at 33.4 km/h based on energy considerations. Finally, the high-speed test was run at 66.7 km/h to equal the equivalent barrier energy of the four lower-speed test repetitions, when accounting for the restitution energy. Table 1 presents the analysis, using true impact speeds. The power-train was expected to influence the vehicle response, so a full frontal high-speed test was run without power-train (Table 2).

Frontal 50% offset tests were carried out repeatedly on the same vehicle to determine shear loads with crush depth. Three test repetitions were run at 33.5 km/h. A high-speed test was conducted at 57.9 km/h and compared to three offset test-repetitions at 33.4 km/h to evaluate the repeated test technique in offset conditions.

The front hood was removed to study power-train kinematics. The dashboard and front seats were removed from all test cars, and lead plates were added to assure that the mass and location of the center of gravity were similar in the test vehicles with power-train. The test mass was 1450 ± 10 kg, except for the test-car without power-train which had a test-mass of 1205 kg.

Following Prasad (1990), a third axle was added to the vehicle floor (Figure 1) to enable the towing of the test-car in the repeated tests. The third axle raised the vehicle-front, and the rear was lifted to adjust the pitch to the original angle. In these tests, the front structure was bent downwards, which impeded the car from being towed. Therefore, the car was raised another 70 mm after the second repetition, and the pitch-angle was adjusted. In all tests, the barrier was mounted and adjusted such that the third load-cell row coincided with the bumper-height.

MEASUREMENTS – All measurements were pre-filtered by SAE J211 filters class 1000 (SAE handbook 1981). The test matrix is presented in Table 2, and the use and purpose of measuring devices are included.

Targets were filmed with 5 high speed (1000 f/s) cameras. One camera filmed the top-view of the vehicle front and compartment to determine the local deformation and yaw of the vehicle. Furthermore, four high-speed cameras (1000 f/s) were located on the sides of the vehicle. Two filmed the (pitch) kinematics of the complete vehicle in each test, and two focussed on the vehicle front structure. Film-analysis showed very low yaw angles during barrier contact (< 0.6 degrees in full frontal and < 6 degrees in offset tests), and the displacement of the top-

Table 1. Repeated test speeds total absorbed energy and total equivalent barrier speed, Mass =1000 kg.

Crash Speed m/s	Crash Speed (km/h)	Kinetic Energy (J)	Coefficient Restitution (Cr)*	Rebound Velocity (km/h)	Absorbed Energy (J)	Total Absorbed Energy (J)	Equivalent Barrier Energy (J)	Equivalent Barrier Speed (m/s)	Equivalent Barrier Speed (km/h)
9.28	33.4	43039	0.2	6.68	41317	41317	43039	9.28	33.4
9.28	33.4	43039	0.1	3.34	42609	83926	84356	13.0	46.8
9.28	33.4	43039	0.1	3.34	42609	126535	126965	15.9	57.4
9.28	33.4	43039	0.05	1.67	42931	169466	169574	18.4	66.7
9.28	33.4	43039	0.05	1.67	42931	212397	212505	20.6	74.2
9.28	33.4	43039	0.05	1.67	42931	255328	255436	22.6	81.4

* coefficient of restitution, Cr = Vreb/Vimp

Table 2. Test matrix, including the use and purpose of measuring devices.

Overlap Amount	Speed (km/h)	Accelero-meters	Interior deformation	Barrier Load cell forces	Vehicle crush	Vehicle motion
Car 1, 100%	66.7	1,2,3	pot-meters o-rings	yes	Top-view camera 2D*	Accelerometer 1
Car 2, 100%	4x33.4	1,2,3	pot-meters o-rings	yes	Top-view camera 2D*	Accelerometer 1
Car 3, 100% no power-train	66.7	1,2,3	o-rings	yes	Top-view camera 2D*	Accelerometer 1
Car 4, 50% hori-zontal	4x33.5	1,2,3	pot-meters o-rings	yes	Top-view camera 2D*	Accelerometer 1
Car 5, 50% hori-zontal	66.7	1,2,3	o-rings	yes	Top-view camera 2D*	Accelerometer 1
Purpose 1 of measurement		validation	validation	-	validation	vehicle motion
Purpose 2 of measurement		deformation (integration)	intrusions	local forces	local crush	local crush
Enables calculation of				front local stiffness		-
Enables calculation of		-	compartment stiffness		-	-

* 2D-mapping technique

Figure 1. Test-car, prepared for repeated tests

center of the vehicle was considered sufficient for deformation measurements. Therefore, the top-view camera was used for analysis of crush characteristics, while the other four cameras were mainly used for the study of vehicle kinematics. Figure 2 shows the targets, which were located in-line with the centers of the load-cells at the bumper and on the roof at B- and C-pillar split.

Three triaxial piezoresistive accelerometers (Endevco, model 7267A, range: [±1500], non-linearity = 2%) were located at 1) the tunnel behind the vehicle rear seat bases, 2) on the driver-side B-pillar floor intersection, and 3) on the passenger-side B-pillar floor intersection. Accelerometer 1 was used to determine car acceleration, speed and displacement time-histories, while accelerometers 2 and 3 provided a second method to estimate yaw and pitch. The car accelerations were filtered post-crash with SAE J211, channel class 60 filters (SAE handbook 1981).

Deformation was determined real-time by double integration of the longitudinal acceleration, and by the top-view film of the car. A vertical projection of the vehicle residual crush was measured post-crash, and compared with the accelerometer and film measurements.

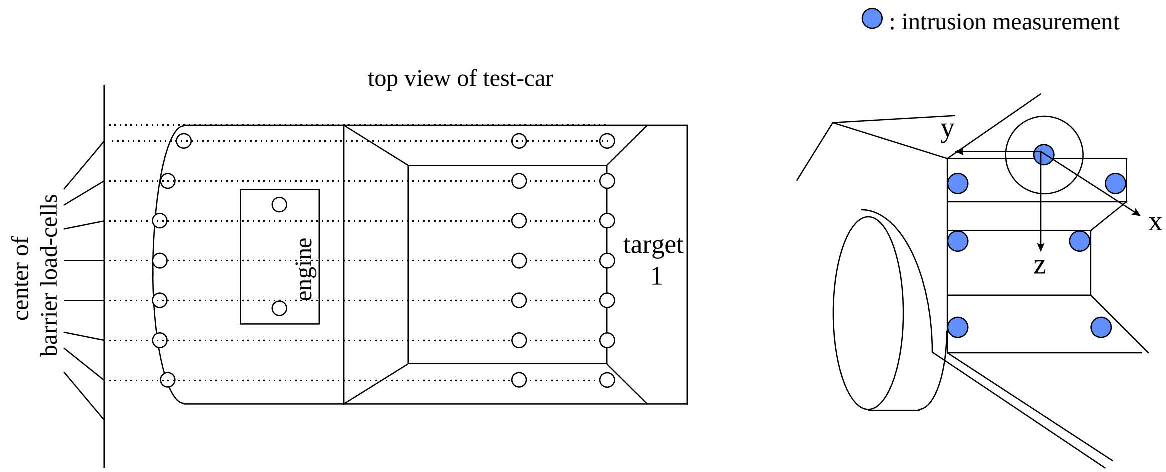

Figure 2. Location of the targets for displacement and intrusion measurements.

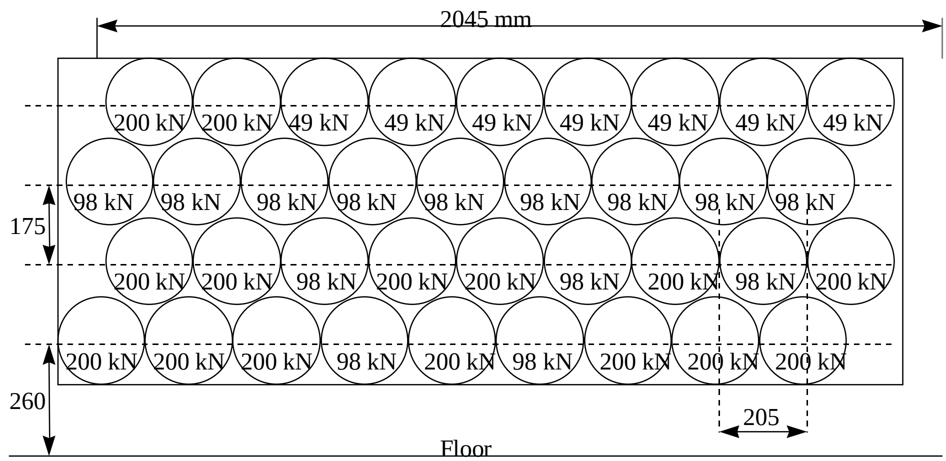

Figure 3. The load-cell barrier with the force range per cell

Local forces were measured real-time by a barrier with 36 load sensors (AC-200), which was manufactured and provided by SAAB Automobile AB. The sensors had a force range of 49, 98 or 200 kN per cell (Figure 3) and had non-linearities between 0.02% and 0.87%. The force time-histories were filtered post-crash with SAE J211 filters, channel class 60 (SAE handbook 1981).

Local longitudinal intrusion was measured real-time by 6 displacement transducers (Novoteknik, series LWG 600, range of 600 mm, maximum acceleration = 100 g's and a non-linearity < 1%) at two locations at the toe-pan, knee-bolster and upper dash board (Figure 2). Rubber O-rings were added to the transducer cylinders to measure maximum local intrusions post-crash. The 3D intrusion of the steering wheel was measured by 3 wire potentiometers (Celesco, type PT101, range=508 mm, accuracy=0.1% and a maximum acceleration of 2,000 g's).

ANALYSIS OF THE TEST DATA

REAL-TIME VERSUS POST-CRASH DATA – The maximum crush and hysteresis were estimated in two ways. Results of the repeated tests had shown that hysteresis slopes were reasonably constant throughout the test repetitions (Figure 5). The maximum crush could therefore be estimated by a linear interpolation of the hysteresis slope from the residual crush upwards until maximum load. Vice versa, maximum crush could be measured from film data, and the hysteresis slope was attained from the line through the residual deformation and the maximum deformation at maximum force.

REPEATED TESTS VERSUS HIGH-SPEED TEST – The deformation after the repeated low-speed tests on one car approximates the deformation in a high-speed crash of equivalent barrier energy (eq. I), in case the front structure has a low rate sensitivity (Warner et al. 1986). Rate sensitivity of the front structure causes higher forces in the high-speed test, and can be approximated by a damping force parallel to the static structural force, F_{struct}. The resulting crush force, F_{crush}, consists of a static structural force, F_{struct}, added by a damping force. The damping force is proportional to the static structural force and velocity Vimp, by a damping coefficient β:

$$F_{crush} = F_{struct}(1+\beta V_{imp}) \qquad \text{(III)}$$

The damping force can be obtained by the difference between crush force at 67 km/h ($F_{crush,67}$) and at 33 km/h (average from 4 repetitions), F $_{crush,33}$, divided by the speed difference:

$$\beta F_{struct} = (F_{crush,67} - F_{crush,33})/(67 - 33) \quad \text{(IV)}$$

The structural force, Fstruct, was approximated by the force measured in the 33 km/h tests, $F_{crush,67}$, so that β was attained by (eq. IV):

$$\beta = \frac{(F_{crush,67} - F_{crush,33})}{F_{crush,33}(67 - 33)} \quad \text{(V)}$$

POWER-TRAIN EFFECT – The passenger compartment and power-train were considered as separate, rigid bodies, connected by an elastic spring, while the behavior of the front structure was estimated by a visco- elasto-plastic spring-damper system. The kinetic energy of the vehicle compartment was absorbed by deformation of the spring-damper system, and its residual deformation determined the barrier force. The more rigid power-train causes the power-train impact forces to be proportional to the impact speed rather than to the power-train residual deformation or displacement.

CALCULATION OF LOCAL LONGITUDINAL STIFFNESS – Local longitudinal force-deflection characteristics were calculated from barrier load-cell forces and post-crash deformation, measured in the repeated tests.

Local intrusions were measured at two locations at toepan, knee and dash level for the driver-side, and were averaged. Barrier forces were measured at corresponding levels, which allowed the calculation of local intrusion stiffnesses. The force-deflection characteristics of the repeated tests were used to minimize the power-train effect on the measured barrier-force.

CALCULATION OF SHEAR STIFFNESS – In offset tests, front stiffness was assumed to consist of longitudinal stiffness and shear stiffness. The longitudinal stiffness was attained from the total stiffness of the corresponding barrier-half measured in the full frontal test. The longitudinal stiffness was subtracted from the measured total stiffness in the offset test to approximate shear stiffness. Data was used from the repeated tests, to reduce power-train inertia effects.

RESULTS

VEHICLE KINEMATICS – The time-histories of vehicle compartment accelerations, deformation, forces and local intrusions were published by Buzeman-Jewkes (1998). These data were provided to enable additional analyses and are valuable for validation purposes. The top-view of the full frontal high-speed test is schematically drawn in figure 4a. Time-histories are shown in figure 4b of the corresponding vehicle acceleration, barrier force, deformation and intrusion.

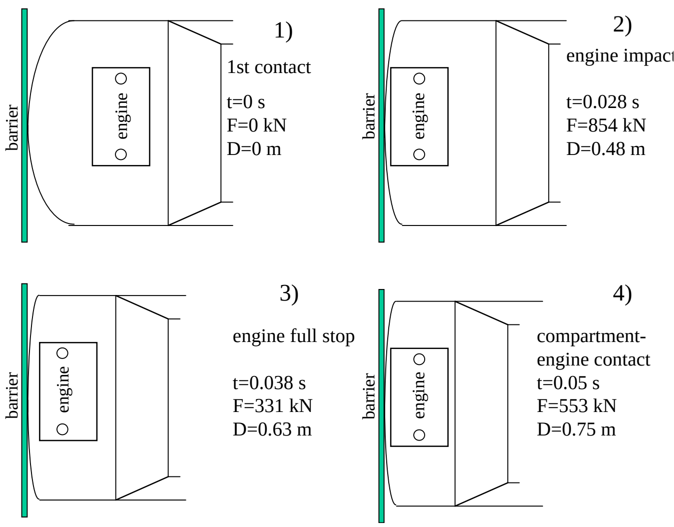

Figure 4a. Top-view of the car in a high-speed in full frontal test at t=0, t=0.028, t=0.038 and t=0.05. The corresponding barrier force and vehicle deformation are included.

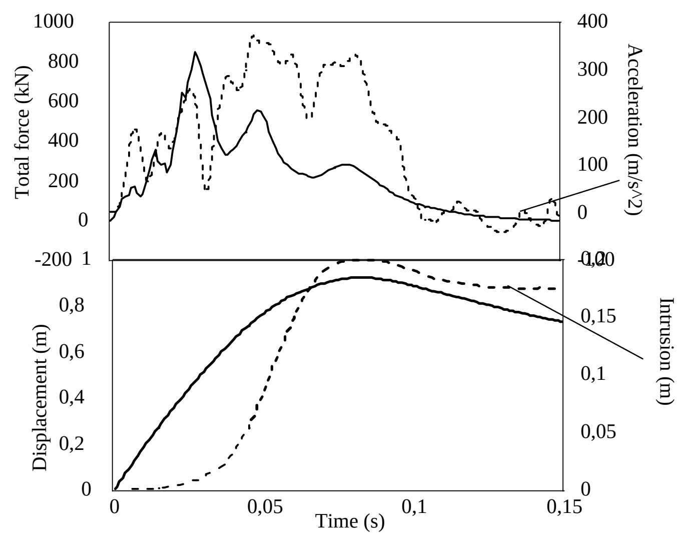

Figure 4b. Time-histories of barrier force, vehicle acceleration, deformation and intrusion in the full frontal high-speed test.

FORCE-DEFLECTION CHARACTERISTICS – Figure 5 shows the force-deflection curves from the full frontal test repetitions. The real-time force deflection (F-D) characteristic could be approximated by curve 1 in the same figure. The barrier force generally increased with crush depth. A higher stiffness was observed for deformation of 0.4-0.45 m, which agreed with the location of the power-train.

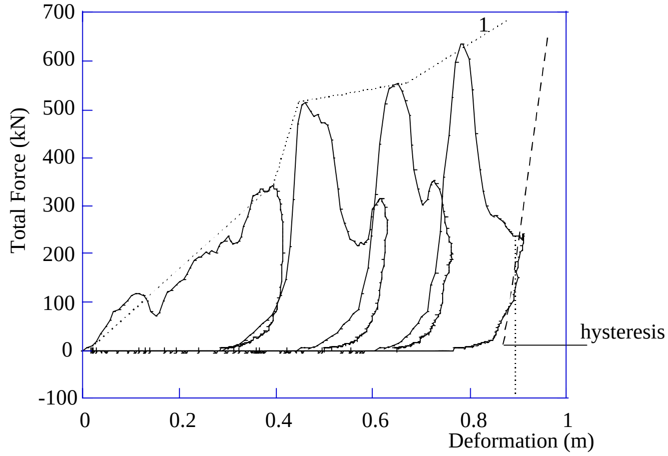

Figure 5. F-D curves of the full frontal repeated crash tests, with curve 1 (. . . . .) an estimated of the stiffness.

REAL-TIME DATA VERSUS POST-CRASH DATA – Post-crash stiffness was estimated using maximum crush (Figure 6a) or hysteresis measurements (Figure 6b), and was represented by curves 2 and 3 respectively. These curves agreed reasonably well with the real-time approximation of curve 1 in Figure 5. However, the power-train impact (deformation 0.4-0.45 m) was not recognized in curves 2 and 3.

Maximum and residual intrusions were measured post-crash, and the values were compared with the corresponding real-time data in Table 3. The results show good agreement, with differences smaller than 10%. Table 4 shows the post-crash measurements of local intrusion in offset crashes.

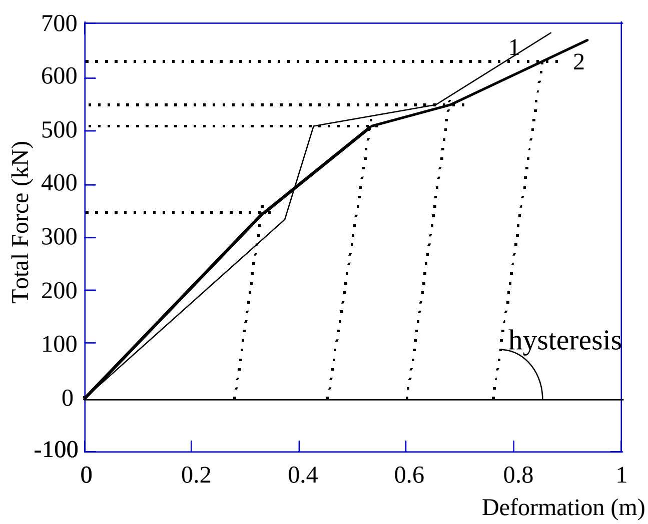

Figure 6a. Comparison between real-time approximation (curve 1) and post-crash data, based on measurement of hysteresis (curve 2)

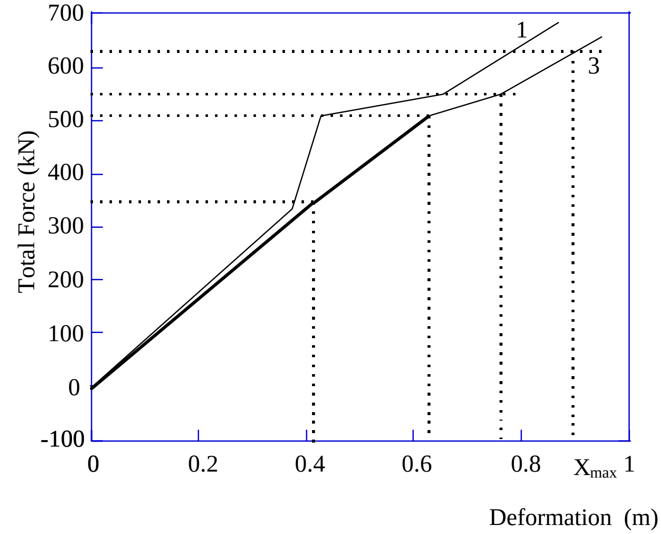

Figure 6b. Comparison between real-time approximation (curve 1) and post-crash data, based on measurement of maximum crush (curve 3)

REPEATED TESTS VERSUS HIGH-SPEED TEST – Figure 7a compares the force-deflection characteristics for the full frontal high speed and repeated tests. The curves were similar up to the maximum deformation of the first test repetition (deformation < 0.4 m). The rate sensitivity factor β was calculated for each 0.05 m vehicle deformation and β had an average and standard deviation of 0.02 $\pm$ 0.025 per (m/s).

Table 3 compares local intrusion for high-speed and repeated full frontal tests. Intrusions were similar at toe-pan level. For knee and dash levels, intrusion was considerably higher in the high-speed test than in the repeated tests.

Figure 7b shows the force deflection curves of all offset tests. The curves in the high-speed test agreed well with those in the repeated crash-tests, and the power-train effect was not as pronounced as in the full frontal tests. The power-train impacted the barrier only partly in the offset configuration.

POWER-TRAIN EFFECT – The inertial effect of the power-train caused higher and longer force-peak in the high-speed test than in the repeated tests at a deformation of 0.45-0.6 m (Figure 7a). The force-peak entails energy, which approximates the higher kinetic energy of the power-train in the high-speed crash. Figure 7c compares the full frontal tests with and without power-train, and clearly shows the power-train effect on the barrier force.

Table 3. Residual and maximum compartment intrusion, measured real-time and post-crash

Full frontal Test	Real-Time (RT) Post-Crash (PC)	Upper Left	Middle Left	Lower Left	Upper Right	Middle Right	Lower Right
Residual Crush (mm)							
Repetition 1	RT	4	5	6	5	3	56
	PC	3	5	6	5	3	6
Repetition 2	RT	23	33	22	26	21	45
	PC	22	33	22	27	22	44
Repetition 3	RT	48	79	72	62	72	156
	PC	45	75	68	57	70	154
Repetition 4	RT	71	131	119	96	130	265
	PC	68	130	121	92	125	246
High-speed	PC	153	190	101	182	154	-
Maximum Crush (mm)							
Repetition 1	RT	15	15	11	19	13	11
	PC	18	17	10	21	13	11
Repetition 2	RT	39	57	31	50	41	65
	PC	37	54	30	56	43	65
Repetition 3	RT	69	108	84	90	102	189
	PC	63	104	78	83	99	182
Repetition 4	RT	100	166	132	128	162	306
	PC	92	160	128	118	155	285
High-speed	PC	191	232	238	229	204	

Table 4. Residual and maximum compartment intrusion, measured post-crash in offset crashes

Offset Test	Upper left	Middle Left	Lower Left	Upper Right	Middle Right	Lower Right
Residual Crush (mm)						
Repetition 1	18	24	8	15	12	11
,, 2	83	108	37	66	60	62
,, 3	224	241	103	166	150	176
High-speed	250	257	134	191	162	214
Maximum Crush (mm)						
Repetition 1	29	41	9	30	23	14
,, 2	116	142	49	97	88	89
,, 3	304	301	131	233	197	220
High-speed	-	327	158	237	198	262

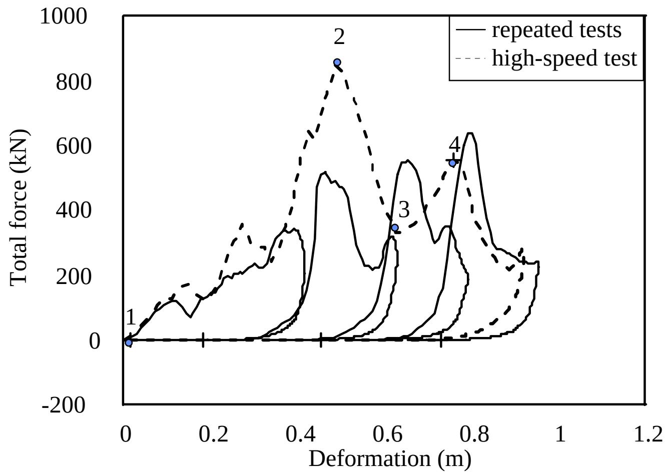

Figure 7a. Comparison of the F-D curves in the high-speed full frontal test with repeated full frontal tests. 1) t=0.0 s, 2) t=0.028 s, 3) t=0.038 s, 4) t=0.05 s

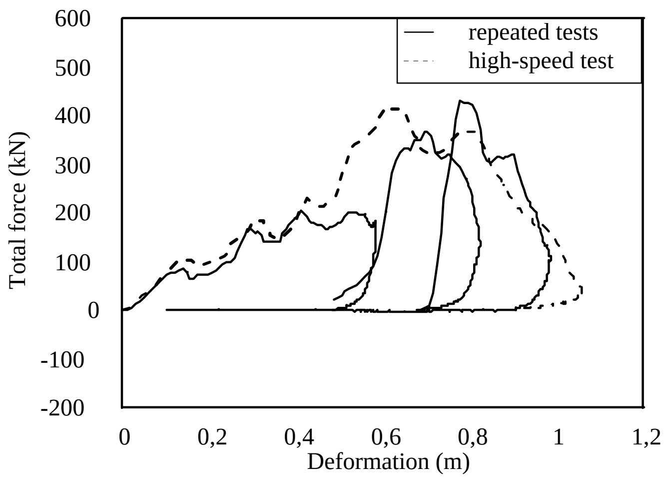

Figure 7b. Comparison of the F-D curves in 50% offset high-speed and repeated tests

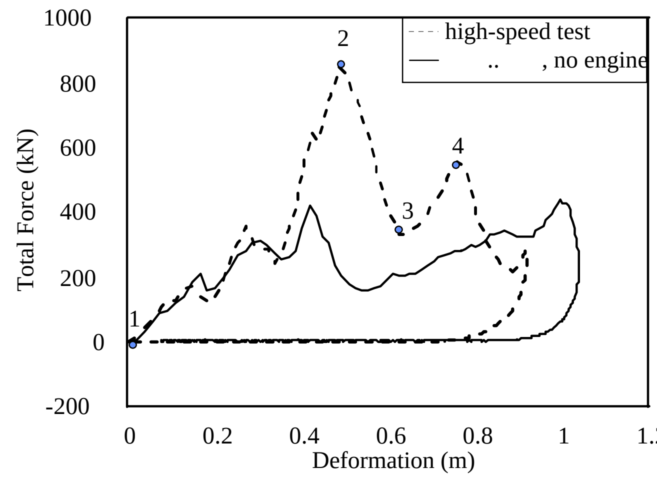

Figure 7c. Comparison of the F-D curves in the high-speed full frontal tests with and without power-train. 1) t=0.0 s, 2) t=0.028 s, 3) t=0.038 s, 4) t=0.05 s

LOCAL LONGITUDINAL STIFFNESS – Figure 8 shows the local maximum forces from the barrier load-cells for each test repetition. In principle, three areas could be distinguished, a) the left and right load-paths (light-gray areas in figure 8a and 8b), b) the power-train (gray area in figure 8c and 8d) and c) the sheet materials (white area).

Figures 9a-c show the intrusion stiffness. At all levels, minimal intrusion (≤ 0.01 m) was observed below a certain force level, followed by a plastic behavior.

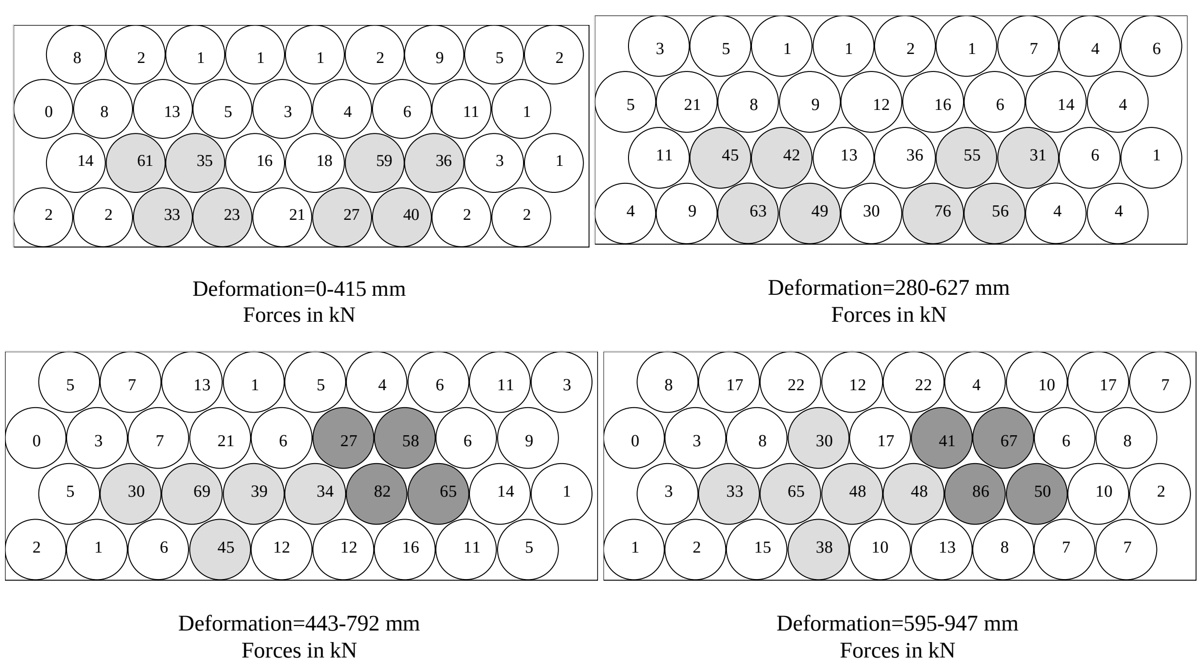

Figure 8. Maps of load-cells with local forces (kN) in each test repetition

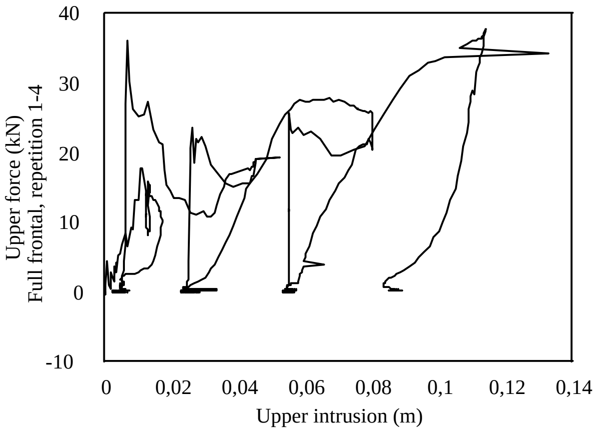

(a) upper (dash) level

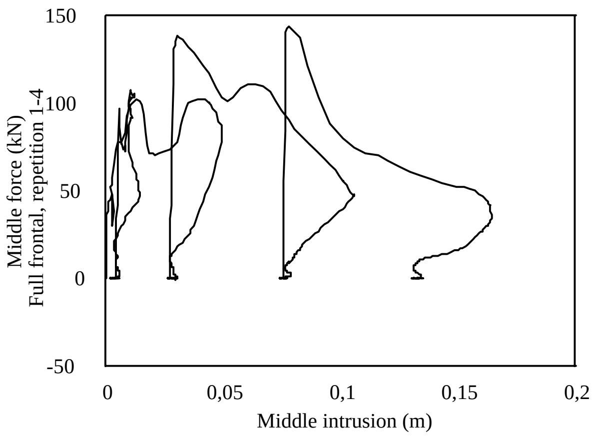

(b) middle (knee) level

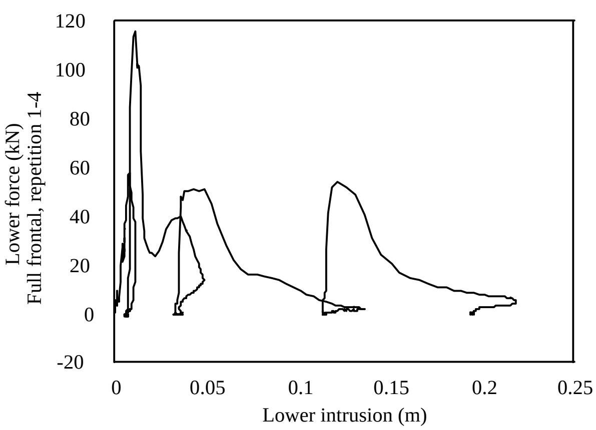

(c) lower (toepan) level

Figure 9. Local intrusion stiffness, measured in repeated tests

SHEAR STIFFNESS – The total barrier force was measured in the repeated offset test and was compared to the total force of the corresponding barrier-half in the full frontal test repetitions (Figure 10). The offset test showed slightly higher forces for deformations between 0-0.2 m, but the load was significantly higher for deformations greater than 0.5 m (Figure 11).

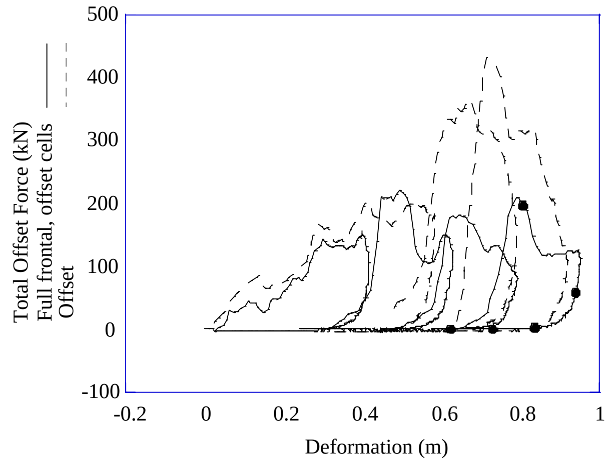

Figure 10. F-D curves of the total force in offset repeated tests vs. that of the total force of 18 corresponding load-cells in full frontal repeated tests.

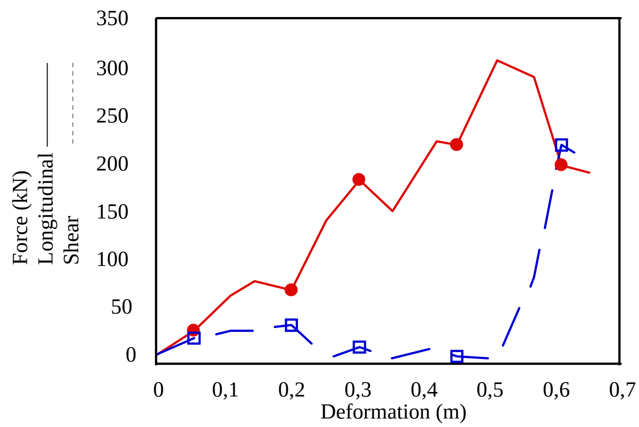

Figure 11. Shear and compression stiffness with deformation

DISCUSSION

A repeated crash test method was combined with a load-cell barrier in full frontal and offset crashes. The purpose of the tests was to determine local longitudinal and shear stiffness of the vehicle front and passenger compartment with vehicle crush. The data also evaluated power-train inertia effects and post-crash measurements in repeated crash tests to estimate front stiffness.

All tests had different impact conditions, which complicated the determination of repeatability. However, the two full frontal high-speed tests show good agreement of the vehicles' force-deflection curves, up to the power-train-barrier contact (Figure 7c). This was an indication of good repeatability, which was confirmed by the similarity of the stiffness curves of the offset tests and the offset load-cells in the full frontal test (Figure 9a).

In full frontal tests, the force characteristics of the vehicle front structure showed visco-elasto-plastic crush behavior (Figure 7c). Figures 4a and 4b compare the vehicle kinematics and responses. The initial stiffness (deformation<0.4 m) involves the crush zone between bumper and power-train (t< 28 ms). A higher stiffness was observed between 0.4 and 0.45 m deformation (28 ms < t < 38 ms), which agreed with the location of the power-train. After the power-train had stopped completely, a plastic response was observed for a deformation greater than 0.45 m (t >38 ms), until the front was fully crushed and a stiffness increase occurred for deformation > 0.7 m (t > 50 ms).

Figure 5 shows an initially high stiffness in tests two to four of the repeated crashes, followed by a force reduction and a second force-peak. In these tests, the power-train impacted the barrier immediately, causing the initial force increase. A force reduction was observed after the power-train had been completely decelerated, and the force increased again when the front was fully crushed. During vehicle unloading, the distance between power-train and compartment was partly restored due to the elasticity of the connecting structure. This may explain the second peak-force in test three.

The residual deformation in the repeated tests agreed well with the corresponding high-speed test. This indicated that vehicle deformation is energy dependent. The repeated test technique could be used to determine the relation between residual crush and impact speed, as concluded by Warner et al. (1986) and Prasad (1990). The repeated test technique has been a useful tool in accident reconstruction.

The barrier-power-train force and passenger compartment intrusion were higher in the high-speed full frontal test. The post-crash deformation data could therefore not be applied directly to calculate vehicle and compartment stiffness. Based on data analysis, the power-train experienced an acceleration of approximately 240 g's, to add 600 kN to the barrier load. The power-train could be considered as a comparatively rigid body, connected by an elastic spring to the compartment, and parallel to the visco- elasto-plastic vehicle structure. Due to the more rigid power-train, barrier-power-train forces were proportional to the power-train impact-speed, and additional kinetic energy of the power-train was manifested as a peak-force (Figure 7a). In modeling or accident reconstruction, the power-train inertia should be modeled parallel to stiffness measurements of the vehicle front structure. Post-crash stiffness data from low-speed (repeated) tests may be a first approximation of front structural stiffness.

The front structure bent down in the repeated tests, but stayed horizontal in the high-speed test. In the latter test, the power-train may have penetrated the passenger compartment at a higher level, and caused the intrusion at knee and dash level.

Local front stiffness was measured. In principle, three stiffness areas could be distinguished, depending on crush depth. In test repetition 1, the left and right load-paths were impacted, which caused the high forces in the light-gray areas of Figure 8a. Test repetition 2 (Figure 8b) involves power-train impact as observed in film (compare with Figure 4a), but the load-paths still absorbed most of the energy. The power-train impact force is seen as the gray area in test 3 (Figure 8c, compare with Figure 4a). The front is deformed up to the firewall (Figure 4a), which distributes the load as reflected by the light-gray area in Figure 8d). Jansson (1982) and Nilsson-Ehle et al. (1982) found a similar force distribution over car width and crush depth.

Shear stiffness could be determined from a comparison between full frontal and offset loads, using the load-cells corresponding to those impacted in an offset test. The estimated shear force varied from 120 kN/m for low deformations (<0.25 m) to 375 kN/m for deformations higher than 0.5 m. The lower shear force may reflect the buckling of the bumper and cross-beam. At higher deformation, the left side of the power-train was impacted and the load was probably transferred to the right side of the car. This may have caused the apparently high shear load. Jansson et al (1982) estimated a shear energy of 13-16 kJ per 30 cm deformation, which corresponds to a shear stiffness of 150-190 kN/m.

The local longitudinal and stiffness data can be used as input for mathematical vehicle models (including dummies) in accident reconstruction and crash safety research. With these stiffness data, a vehicle model could be developed to estimate vehicle acceleration and passenger compartment intrusion in various frontal crash conditions. Variations in vehicle stiffness characteristics could be made and the effect on occupant (dummy) injuries studied. Compatibility research could benefit from such a simple but valid model.

CONCLUSION

- Low-speed, repeated tests well approximate the car deformation in a high-speed crash of similar equivalent barrier speed. The tests are therefore useful for investigations of both high and low-speed crashes.
- The power-train inertia affect bumper-force and compartment intrusion significantly. The power-train can be considered as a separate rigid front body.
- Local longitudinal front stiffness can be measured by full frontal repeated tests against a load-cell barrier.
- Front shear stiffness can be attained from repeated offset tests with a load-cell barrier. The barrier force in the offset tests minus that of the corresponding barrier half in full frontal tests is a reasonable estimate for the shear force.
- Local intrusion stiffness can be estimated in frontal repeated tests from the barrier load-cell forces and local compartment intrusions.
- The new test method provides local stiffness data that are valuable for accident reconstruction investigations, especially for non-distributed frontal crashes. The data can also be used as input for a tool in compatibility research. The test-method assesses stiff-

ness and mass aggressivity. Further research would benefit from testing various car models, using the presented method.

ACKNOWLEDGMENTS

This research was sponsored by the Swedish National Road Administration and by Saab Automobile AB (Sweden). The authors would like to thank Autoliv (Sweden) for the use of their crash-test facilities, and Brent Benson (Benson Engineering, USA) for his expertise and fruitful suggestions concerning the repeated crash-test method.

REFERENCES

1. Buzeman-Jewkes, D.G. (1998) Local Longitudinal and Shear Stiffness of the Vehicle Front, and Vehicle Responses in Repeated and High-Speed Crash-tests. Internal Report No. 1998-08-17, Department of Machine and Vehicle Design, Crash Safety Division, Chalmers University of Technology, Gothenburg, Sweden
2. Campbell, K. L. (1974) Energy Basis for Collision Severity. Procs. of SAE Conf. Warrendale, MI. Paper No. SAE 740565, pp. 1-13
3. Hobbs, C. A.; Williams, D. A.; Coleman, D. J. (1996). Compatibility of Cars in Frontal and Side Impact. Procs. of the 15th Conference on Enhanced Vehicle Safety, Paper No. 96-S4-O-05, pp. 617-625, Melbourne, Australia.
4. Jansson U. (1982) Energy Based Determination of Speed in Underride Impacts. Graduation Report, Chalmers University of Technology, Gothenburg, Sweden
5. Nilsson-Ehle, A.; Norin, H.; Gustafsson, C. (1982) Evaluation of a Method for Determining the Velocity Change in Traffic Accidents, Procs of the 9th Int. Conf. on ESV, pp 741-750
6. Prasad, A. K. (1990) Energy Dissipated in Vehicle Crush - A Study Using the Repeated Test Technique. Procs. SAE Conf. Warrendale MI. Paper NO. SAE 900412, pp. 17-27
7. Warner, C.Y.; Allsop, D.L.; Germane G.J. (1986) A Repeated Crash Test Technique for Assessment of Structural Impact Behaviour", Procs. of SAE Conf., Warrendale, MI. Paper No. SAE 860208, pp 193-209.